2013 IEEE International Conference on Robotics and Automation (ICRA)
Karlsruhe, Germany, May 6-10, 2013

Towards Automated Optoelectrowetting on Dielectric Devices for Multi-Axis Droplet Manipulation

Vasanthsekar Shekar, Matthew Campbell, and Srinivas Akella

Abstract— **Lab-on-a-chip technology scales down multiple laboratory processes to a chip capable of performing automated biochemical analyses. Electrowetting on dielectric (EWOD) is a digital microfluidic lab-on-a-chip technology that uses patterned electrodes for droplet manipulation. The main limitations of EWOD devices are the restrictions in volume and motion of droplets due to the fixed size, layout, and addressing scheme of the electrodes. Optoelectrowetting on dielectric (OEWOD) is a recent technology that uses optical sources and electric fields for droplet actuation on a continuous surface. We describe an open surface light–actuated OEWOD device that can manipulate droplets of multiple volumes ranging from 1 to 50 μL at voltages below 45 V. To achieve lower voltage droplet actuation than previous open configuration devices, we added a dedicated dielectric layer of high dielectric constant (Al_2O_3 with ε_r of 9.1) and significantly reduced the thickness of the hydrophobic layer. The device is capable of transporting droplets at speeds as high as 12 mm/sec using a data projector as an optical source. We developed a multiple axis contact pad design to apply lateral electric fields along different axes to achieve multi-axis droplet movement. We demonstrated microfluidic operations including droplet merging, mixing, and parallel droplet motion. Further, the OEWOD device is capable of droplet transportation using a tablet computer's LCD screen as an optical source.**

I. Introduction

Lab-on-a-chip technology scales down multiple laboratory processes to chips capable of performing automated chemical analyses. A distinct benefit of miniaturized lab-on-a-chip systems is the significant reduction in sample consumption and increase in throughput [1]. Digital microfluidics deals with the manipulation of discrete droplets of chemicals [2], [3]. Droplet manipulation technologies include electrowetting, dielectrophoresis, surface acoustic waves, thermocapillary forces, magnetic forces, and optical forces [4]. Among these methods, electrowetting provides the advantages of fast response time, easy implementation, and large forces from the millimeter to micrometer scales. Electrowetting is the modification of the wetting properties of a surface by the application of external voltage. The concept of electrowetting was first introduced by Beni and Hackwood [5]. Digital microfluidic devices that use electrowetting for droplet movement are called *electrowetting on dielectric* (EWOD) devices. The main limitations of EWOD devices are the restriction in the droplet volume based on the size of the electrode, the constraints on the droplet motions from the layout of electrodes, and layout design restrictions arising from electrode addressing constraints. We can overcome these limitations by light-actuated droplet manipulation.

Optoelectrowetting (OEW) is a light-actuated droplet manipulation technique using optical sources and electric fields. A projected pattern of light, which acts as a virtual electrode, is moved to manipulate the droplet. The optical source generating the patterns ranges from a laser [6] to an LCD screen [7]. The main advantages of OEW devices are the simplicity in fabrication process and the large continuous droplet manipulation region compared to EWOD devices. Devices that use OEW on a dielectric surface for droplet manipulation are called *optoelectrowetting on dielectric* (OEWOD) devices. OEWOD devices can be further classified into open surface devices and sandwiched configuration devices based on the number of substrates used and the application of the electric field. Sandwiched configuration devices use two parallel substrates to manipulate droplets sandwiched between the substrates. Open surface devices use a single substrate and lateral electric fields for droplet manipulation. Open surface designs make it easy to interface the OEWOD device with other microfluidic structures (such as on-chip reservoirs) to increase its versatility for biochemical analyses [8].

In this paper, we present an open surface OEWOD device that significantly improves upon the performance of previously reported open surface devices [4]. We increase the effective capacitance of the dielectric region by adding a dedicated dielectric layer (Al_2O_3, 25 nm) of high dielectric constant (ε_r of 9.1) and reducing the thickness of the hydrophobic layer, compared to recently reported open surface devices [7]. By increasing the effective capacitance, the threshold voltage was reduced from a few kilovolts [7], [4] to 40.9 V. Low voltage multi-axis droplet manipulation was successfully demonstrated by a multiple-axis contact pad layout surrounding the droplet manipulation region. The device is capable of performing multi-axis droplet motion at speeds as high as 12 mm/sec with a data projector as an optical source. It can perform operations such as mixing, merging, and parallel droplet manipulation. Further, the OEWOD device is capable of droplet transportation using a tablet computer's LCD screen as an optical source. The significant reduction in droplet actuation voltage along with the enhanced capability of low voltage multi-axis manipulation using this OEWOD device is a step towards achieving a portable light-actuated microfluidic device.

This work was partially supported by National Science Foundation Award IIS-1019160.

V. Shekar, M. Campbell, and S. Akella are with the University of North Carolina at Charlotte, Charlotte, North Carolina 28223. vasanthshekar@gmail.com, mcampb51@uncc.edu, sakella@uncc.edu

II. Related Work

There has been great interest in optical manipulation of objects for robotics and automation applications. The majority of the work has focused on the use of optical tweezers to manipulate cells and beads for biology applications [9], [10], [11], [12], [13]. In this paper, we focus on optical manipulation of droplets for lab-on-a-chip devices.

Light-actuated droplet manipulation can be achieved using several methods like direct optical force actuation [14], [15], optothermal actuation [16], [17], and optoelectronic actuation [6], [10]. Among these methods, optoelectrowetting (OEW) is effective due to its fast response, ease of implementation, and reliability. An OEW device is coated with a featureless photoconductive layer followed by an insulating dielectric layer and a hydrophobic layer. Dark regions of projected light act as virtual electrodes to manipulate the droplets. OEW devices were first reported by Chiou *et al.* [6] who used laser beams (65 mW/cm^2) with discrete electrodes for droplet manipulation.

Recent work in optically activated microfluidic devices has focused on reducing the droplet actuation voltage and optical source intensity. Pei *et al.* [18] reported a light-actuated droplet manipulation (LADM) device in which the optical source is a conventional data projector (DELL 4210X) instead of a laser. The aggressive scaling of the dielectric thickness in the device fabrication helps them achieve high speed droplet manipulation (2 cm/sec) in low optical intensity (3 W/cm^2).

Park *et al.* [7] reported a *single-sided continuous optoelectrowetting* device (SCOEW) that uses a data projector for droplet actuation. They applied lateral electric fields using aluminum contact pads. The lateral electric field enables droplet manipulation based on the relative ratio of photoresistances rather than their absolute values. This unique property allows the optical actuation of droplets with low optical intensity sources (e.g., LCD screen). The SCOEW device is an open surface configuration, and Park *et al.* successfully integrated on-chip reservoirs. The main limitation of the SCOEW device is that it requires high voltage (a few kilovolts [4]) for droplet actuation. In this paper, we present an OEWOD device that significantly improves upon the performance of the previously reported open surface devices [4].

Since the droplets can be manipulated anywhere in the active region, there can be undesired droplet collisions. Hence, motion planning of droplets plays a critical role in light-driven droplet manipulation systems. Droplet coordination and scheduling on digital microfluidic systems has been previously explored only for EWOD devices [19], [20], [21]. Recently Ma and Akella [22] presented algorithms for the problem of coordinating multiple droplets in light-actuated digital microfluidic systems. They mainly focused on creating matrix formations of droplets by parallel manipulation.

III. Design and Fabrication

The design of our fabricated OEWOD device is shown in Figure 1. We designed it to have multiple contact pads to create lateral electric fields along multiple axes. A photoconductive film of hydrogenated amorphous silicon (a-Si:H, 0.5 μm) layer is deposited using Plasma Enhanced Chemical Vapor Deposition (PECVD). The contact pads are fabricated by depositing gold (100 nm) using electron beam deposition. A thin film of dielectric aluminum oxide (Al_2O_3, 25 nm) is deposited using atomic layer deposition (ALD). The substrate is spin coated with a hydrophobic layer of 2% Teflon (1:2, 6% TeflonAF:Flourinert FC40, 250 nm) at 3000 R.P.M for 60 seconds and post baked at 160°C for 10 minutes.

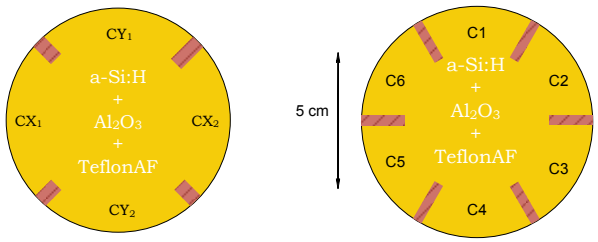

(a) (b)

Fig. 1. Schematic top view of a multiple axis OEWOD device. The droplet manipulation region (shaded) consists of a photoconductive layer (a-Si:H), dielectric layer (Al_2O_3), and hydrophobic layer (2% TeflonAF). (a) A four contact pad layout in which the contact pads CX and CY (in yellow) are for applying external voltage in the horizontal and vertical directions respectively. (b) A six contact pad layout in which C1 to C6 are the contact pads for applying external voltage.

IV. Working Principle

The working principle of the OEWOD device can be explained using its equivalent circuit model [7], shown in Figure 2. The photoconductive layer (a-Si:H) is modeled as resistances R_1, R_2, R_3, R_4 connected in series. The capacitances C_1 to C_3 are modeled as the effective capacitance across the dielectric and hydrophobic layers.

When droplets are introduced on the device, the contact angle with the surface is greater than 90° due to the hydrophobic nature of the device surface. When the device is uniformly illuminated by light, the applied voltage drops linearly across the resistors. As a result, the voltage drops across capacitors C_1 and C_3 are equal and the droplet does not experience any contact angle change.

We will refer to a user specified dark region in the projected optical pattern as a *virtual electrode*. When a portion of the droplet is illuminated by bright light and the remaining portion is dark (due to the virtual electrode), the photoresistances R_1, R_2, and R_4 have low resistance due to bright illumination whereas R_3 has high resistance due to low illumination. As a result, the voltage drop across the capacitors C_1 and C_2 will be low due to low voltage drop across R_1 and R_2 respectively. Consequently, the voltage drop across C_3 will be high due to high voltage drop across R_3. When there is a voltage drop V across a capacitor with capacitance C, it induces a charge Q, where $Q = C.V$. Let the charge buildup across C_1, C_2, and C_3 be Q_1, Q_2, and Q_3 respectively. Since the voltage drop across C_3 is greater than C_1 and C_2, Q_3 will be greater than Q_1 and Q_2.

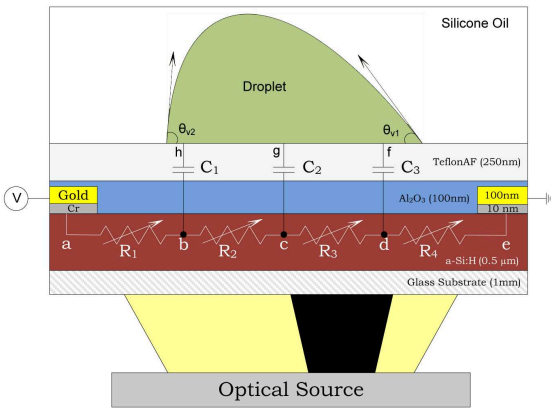

Fig. 2. Circuit behavior when there is bright illumination at one end of the droplet (region under R_1 and R_2) and a dark virtual electrode at the other end of the droplet (dark region under R_3). R_1, R_2, and R_4 have low resistance due to bright illumination and R_3 has high resistance due to the dark region. Figure not drawn to scale. Based on [7].

The electrostatic force associated with the accumulated charges acts to oppose the surface tension of the droplet at the solid–liquid interface [3], [2]. As a result, the surface tension is reduced and causes enhanced droplet wetting at the droplet end near C_3 (Figure 2). The relation between the droplet contact angle change and the voltage across the dielectric layer is given by the Young–Lippmann equation [3]:

$$\cos\theta_V = \cos\theta_0 + \frac{1}{2\gamma}CV^2 \qquad (1)$$

where θ_V and θ_0 are the contact angles of the droplet with voltage V and zero voltage respectively, γ is the surface tension at the solid (device)-liquid (droplet) interface, and C is the capacitance per unit area across the dielectric region. The difference in contact angle creates a pressure gradient, which leads to the bulk flow of the droplet towards the non-illuminated region [2], [7].

V. Laboratory Setup

The experimental setup for droplet actuation on the OEWOD device is shown in Figure 3. The device is immersed in a silicone oil medium (Polydimethylsiloxane trimethylsiloxy-terminated, 1.0 cSt) inside a transparent Petri dish. A commercial data projector (Dell 4210X) was used as the optical source. A commercial web camera (Logitech C910) was used for recording the droplet movements. The external voltage was applied using a Trek 2205 voltage amplifier powered by a EZ GP-4303D adjustable DC power supply. The droplets were introduced on the OEWOD device using a Hamilton microliter syringe.

A. Optical Pattern Generation for Droplet Manipulation

Optical patterns are generated using a JavaScript application. The application is highly portable and can be used on any modern mobile device or desktop computer with an Internet browser. There are settings for the user to easily add or remove virtual electrodes and change various characteristics including size and speed. Virtual electrodes

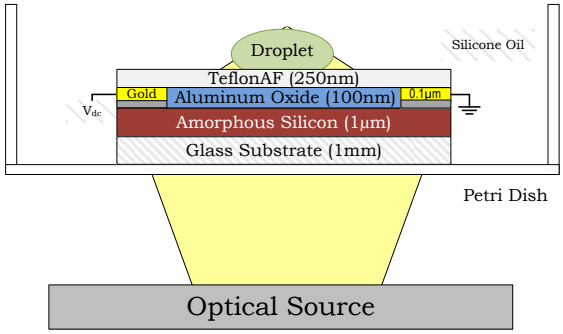

Fig. 3. Side view of the OEWOD device laboratory setup. A camera is stationed above the OEWOD device to record the droplet movement. Figure not drawn to scale.

can be individually or collectively selected and moved using a keyboard. Virtual electrodes can also be generated and manipulated using programmed instructions. The instructions make it possible to perform multiple droplet motion in parallel along multiple axes. Instructions control virtual electrode shape, orientation, and precise movement timing. Algorithms to perform optimized droplet operations [22] can automatically generate precompiled instructions.

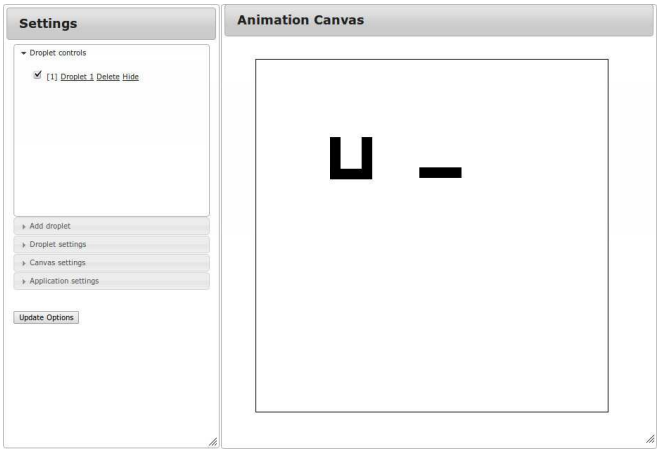

Fig. 4. Graphical user interface for controlling the optical patterns; a U-shaped electrode and rectangular electrode are shown. The settings menu controls the size, shape, speed, and color of the optical patterns. The values specified are in pixels. The animation canvas is the region where the optical patterns are drawn and moved using a keypad or as programmed.

VI. Experimental Results and Analysis

The fabricated OEWOD devices are capable of performing operations including droplet transportation, merging, multi-axis movement, parallel manipulation, and multi-volume droplet manipulation [23]. The *active region* of an OEWOD device is the area where droplets can be manipulated using optical patterns (Figure 5). The external voltage is applied at the contact pads shown in Figure 1. We used water droplets in a silicone oil medium.

A. Reduction in Threshold Voltage

Recent work in optical microfluidics has focused on achieving a portable microfluidic system [4]. Reduction in

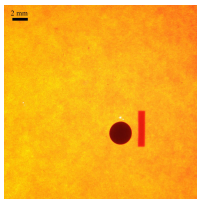

Fig. 5. Top view of the OEWOD device active region. The droplet can be manipulated anywhere in the active region by a virtual electrode (dark rectangle next to the droplet).

threshold voltage is a key parameter to create a portable system that can be powered by portable batteries.

To reduce the threshold voltage (V_{th}) from previously reported devices [4], a designated dielectric layer (Al_2O_3) of high dielectric constant (ε_r of 9.1) was included in the fabrication process. By including Al_2O_3, we successfully reduced the threshold voltage from a few kilovolts reported in [4] to 40.9 V DC. To experimentally analyze the significance of the dielectric layer, different sets of devices with different thicknesses of Al_2O_3 were fabricated. Analysis shows that increasing the dielectric constant of the dielectric layer and coating a thinner hydrophobic layer reduces the threshold voltage. By varying the Al_2O_3 thickness we experimentally verified this for our OEWOD devices and successfully reduced the threshold voltage to 40.9 V DC.

B. Influence of Device Capacitance on Droplet Speed

The net force F_{net} acting on the droplet is proportional to the capacitative energy per unit area stored in the dielectric layer [18] and is given by

$$F_{net} \simeq \frac{\varepsilon}{D} V^2 \tag{2}$$

where ε is the effective dielectric constant across the device, D is the thickness of the dielectric layer, and V is the voltage drop across the dielectric layer. High dielectric constant materials can increase the net force on the droplet [24], thereby increasing the droplet speed. We fabricated devices with two different dielectric thicknesses (D_{25} with 25 nm Al_2O_3, and D_{10} with 10 nm Al_2O_3). Our experiments show that the average droplet speed is higher in device D_{25} than device D_{10}. The fabricated OEWOD device has transported droplets at speeds up to 12 mm/sec (at 120 V DC).

C. Variation in Contact Angle

When there is uniform illumination under the droplet, the contact angle remains the same at both ends of the droplet (Figure 6(a)), and it is approximately 150°. When the region under the droplet is illuminated by a dark region and the remaining region by bright light, the contact angle is reduced at both the ends, due to equal illumination at the droplet ends. Figure 6(b) shows the contact angle reduced to 120° at both ends of the droplet. When a portion of the droplet is illuminated by the dark region and the remaining region by bright light, the droplet's contact angle is reduced in the dark region thus creating a contact angle difference $\Delta\theta$.

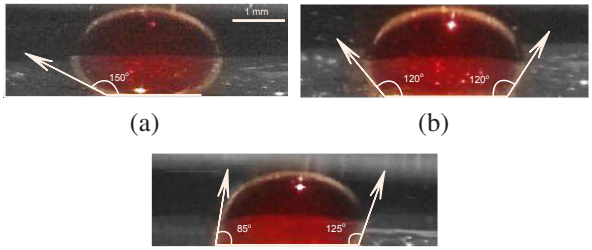

Fig. 6. A droplet showing contact angle variations under different illumination conditions. (a) When the active region has uniform illumination, the droplet contact angle remains unchanged (150°). (b) When the region under the droplet is dark and the remaining active region is illuminated by bright light, the contact angle reduces at both ends (120°). (c) When a portion of the droplet has a dark region (virtual electrode) and the remaining region has bright light, the contact angle significantly decreases at the end with the dark region (85°).

Figure 6(c) shows the measured contact angles at the ends of the droplet (125° and 85°) and a $\Delta\theta$ of approximately 40°.

D. Influence of Virtual Electrode on Droplet Motion

1) Virtual Electrode Shape: We observed that the droplets may move off the virtual electrode due to lateral drift. To avoid this, we experimented with different virtual electrode shapes. The U-shaped virtual electrode (Figure 9) in particular, reduces sideways drift of the droplet while moving and thus prevents uncontrolled droplet movement.

2) Virtual Electrode Dimensions: In the OEWOD device, for a specified droplet volume, droplet movement is influenced by the actuation voltage, intensity of the optical source, and the dimensions of the virtual electrode. While keeping the actuation voltage (80 V DC) and the optical source constant, we modified the width of a rectangular virtual electrode to analyze the droplet behavior. Experiments were conducted by changing the dark band width while keeping the droplet volume constant.

Case A: Virtual Electrode Width $<$ Droplet Radius. If the virtual electrode width is significantly smaller than the droplet radius as shown in Figure 7(a), only a small portion of the droplet region overlaps the dark region. Improved wetting due to optoelectrowetting was exhibited only on the overlapping droplet region. So there will not be sufficient reduction in contact angle in the dark band region of the droplet to generate movement.

Case B: Virtual Electrode Width $\simeq$ Droplet Radius. If the virtual electrode width is approximately equal to the droplet radius as shown in Figure 7(b), then half of the droplet will be illuminated by bright light and the other half will be illuminated by the dark region. The droplet's contact angle under the dark region decreases due to optoelectrowetting and the contact angle of the droplet in the bright region remains unchanged. This difference in contact angles at the ends of the droplet helps the droplet move towards the wetting region (i.e., towards the virtual electrode).

Case C: Virtual Electrode Width $>$ Droplet Radius. If the virtual electrode width is greater than the droplet radius as

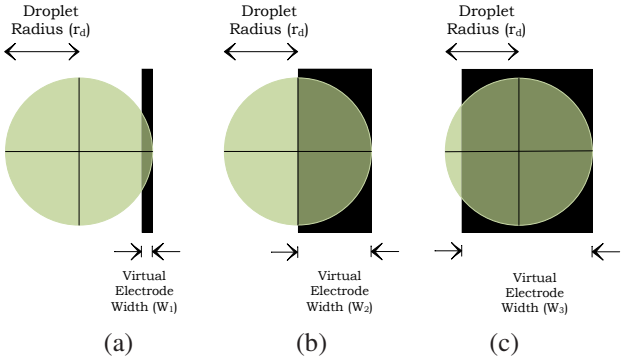

Fig. 7. Relation between droplet radius and virtual electrode width. (a) Droplet radius is significantly larger than the width of the virtual electrode ($r_d > W_1$). (b) Droplet radius is equal to the width of the virtual electrode ($r_d \approx W_2$). (c) Droplet radius is significantly smaller than the width of the virtual electrode ($r_d < W_3$).

shown in Figure 7(c), then most of the droplet will be covered by the dark region. The droplet contact angle changes at both ends of the droplet, but the difference in contact angles will be small. Hence no droplet movement is observed.

The experimental results in Table I show that the droplet moves continuously when the virtual electrode width is approximately equal to the droplet radius. The droplet stops moving as the difference between the virtual electrode width and the radius starts increasing. The analysis was also experimentally verified using 10 μL droplets.

E. Multi-Axis Droplet Manipulation

We developed a multi-axis contact pad design to achieve a strong electric field along different axes by activating different sets of contact pads. Park *et al.* [25] reported that droplet transportation is difficult in the direction perpendicular to the applied electric field due to weak electric field strength. They used optical patterns of different shapes (Paired-Diamond) to increase the electric field strength in two perpendicular directions for achieving multi-axis droplet motion at high voltages [8]. We achieve low voltage multi-axis motion without modifying the shapes of the optical pattern. We instead fabricated multiple contact pads around the active region (Figure 1).

For a given pair of activated contact pads, the droplet can be moved at different angles as shown in Figure 8. We observed droplet motion up to 60° from the axis of activated contact pads without a significant change in droplet speed. A droplet (20 μL) was moved along the vertical direction and then the virtual electrode orientation was changed by 45°. The droplet was moved along the new direction at the same speed and voltage. To further demonstrate the capability of the device, the droplets were manipulated at multiple angles on either side of the activated contact pads as shown in Figure 9. Initially, a droplet (20 μL) was moved at 30° (clockwise) with reference to the activated contact pad axis followed by motion 30° and 60° (anticlockwise) with reference to the axis of activated contact pads. By activating different sets of contact pads at different instants, we can manipulate droplets at arbitrary angles and directions.

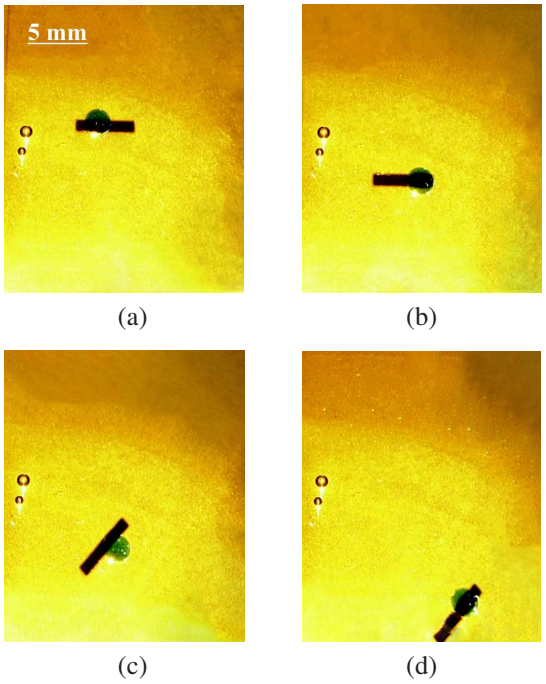

Fig. 8. Multi-axis droplet movement using a rectangular virtual electrode. The activated contact pads C1 and C4 are positioned as in Figure 1(b). The droplet volume is 20 μL. (a) Initial position of droplet. (b) Droplet has been moved along the axis of activated contact pads. (c) Angle of virtual electrode is changed to 45°. (d) Droplet after motion along the new direction.

F. Droplet Manipulation using LCD Screens

We demonstrated droplet manipulation on a TFT LCD screen (Samsung Galaxy Tab 10.1 tablet) using the OEWOD device at an input voltage of 567.2 V DC and droplet speed of 1.2 mm/sec. Previously reported OEW devices use a few KV for manipulating droplets using LCD displays [4]. The improvement in effective device capacitance helped us reduce the actuation voltage and improve droplet speed. We used 50 μL droplets and a 5 mm wide virtual electrode to transport the droplet (Figure 10). This reduction in voltage requirement for droplet manipulation using portable low intensity optical sources takes us a step closer towards achieving a portable microfluidic system.

G. Droplet Operations

We demonstrated microfluidic operations including droplet merging (Figure 11) and parallel droplet movement (Figure 12) using the OEWOD device with a data projector. Merging was tested on 10 μL and 20 μL droplets. We observed that the merging is instantaneous once the droplets come close to each other. The mixing of a merged droplet is completed by moving it in both vertical directions from its merged location. Figure 12 shows the simultaneous parallel motion of two droplets. Two droplets of 20 μL are simultaneously transported at approximately 2.5 mm/sec. This ability to actuate droplets in parallel at equal voltage and speeds can potentially play a key role in performing biochemical analyses for biological applications.

TABLE I

INFLUENCE OF VIRTUAL ELECTRODE DIMENSION ON DROPLET MOTION. THE DROPLET VOLUME IS KEPT CONSTANT AND THE VIRTUAL ELECTRODE DIMENSION IS VARIED IN EACH CASE TO OBSERVE THE DROPLET BEHAVIOR.

Droplet size		**Virtual electrode width**		**Droplet radius / Virtual electrode width**	**Droplet Behavior**
Volume (μL)	**Radius** (mm)	(pixels)	(mm)		
20	1.75	10	0.9	1.94	No contact angle change
20	1.75	20	1.8	0.97	Continuous droplet movement
20	1.75	25	2.2	0.79	Contact angle changes, no droplet movement
20	1.75	30	2.7	0.65	No contact angle change

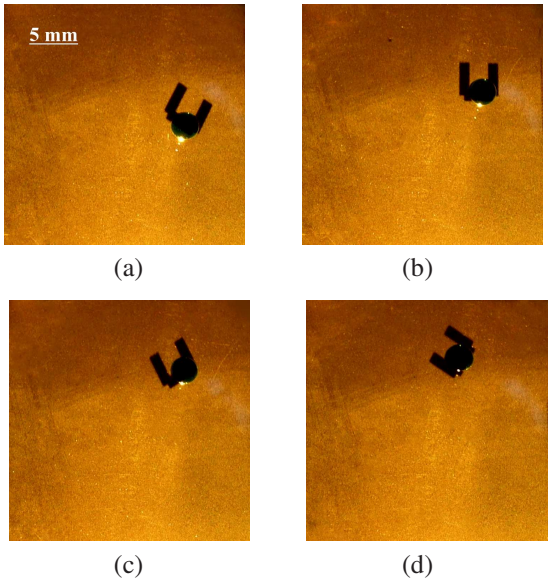

Fig. 9. Multi-axis droplet movement using a U-shaped virtual electrode. The activated contact pads C1 and C4 are positioned as in Figure 1(b). (a) Droplet moving 30° clockwise with reference to the axis of activated contact pads. (b) Droplet moves along axis of activated contact pads. (c) Droplet moving 30° anticlockwise with reference to the axis of activated contact pads. (d) Droplet moving 60° anticlockwise with reference to the axis of activated contact pads.

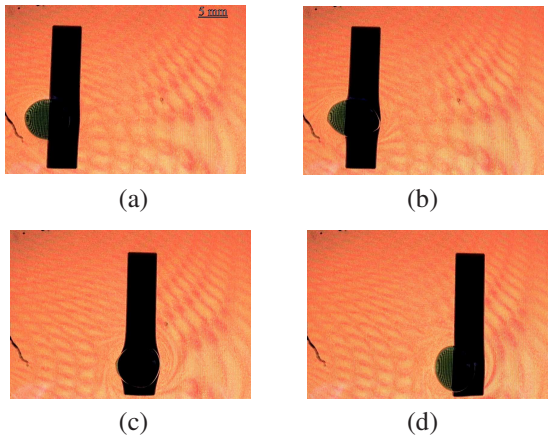

Fig. 10. Droplet movement using a Samsung Galaxy Tab tablet as the optical source. The contact pads C1 and C4 are activated and positioned along the direction of droplet motion. (a) Initial position of droplet (70 μL). (b) The contact angle of droplet changes and droplet starts moving. (c) Droplet at intermediate position. (d) Final destination of the droplet.

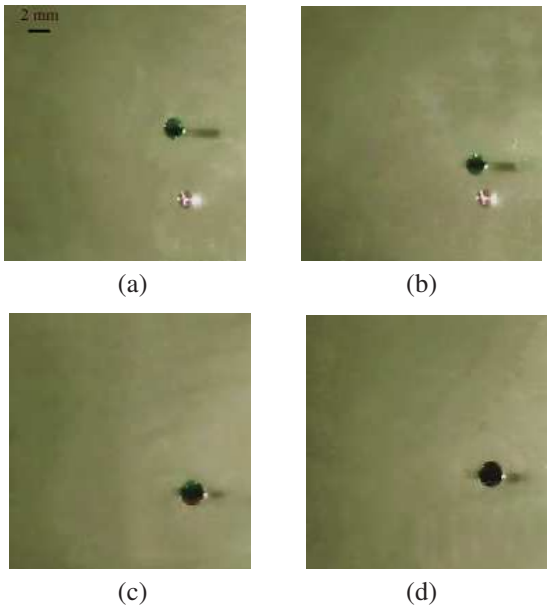

Fig. 11. Droplet mixing. (a) The initial position of two colored (green and red) droplets (10 μL each). (b) The green droplet has moved towards the red droplet, which is kept stationary in its initial position. (c) Once the red and green droplets are merged, the upper portion of the merged droplet remains green and the lower portion remains red. (d) The mixed droplet after it has been moved in both vertical directions.

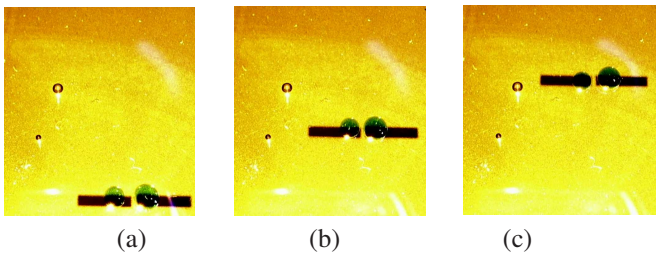

Fig. 12. Parallel motion in an OEWOD device. Two droplets are transported simultaneously by virtual electrodes moving at 3 mm/sec.

VII. CONCLUSION

A. Contributions

In this paper, we presented an open surface optoelectrowetting microfluidic device that can manipulate droplets of multiple volumes ranging from 1 to 50 μL at voltages as low as 40.9 V DC, and capable of transporting droplets at speeds as high as 12 mm/sec. We achieved this low voltage activation by adding a dedicated Al_2O_3 dielectric layer of high

dielectric constant and significantly reducing the thickness of the hydrophobic layer. The advantages of this device are low voltage droplet actuation and multi-axis droplet motion. This device can perform basic digital microfluidic operations such as transportation, mixing, and merging at low voltage and we demonstrated multi-axis droplet motion at equal speeds. We also described the effect of the relation between the optical pattern dimensions and the droplet size on droplet behavior. Finally, we demonstrated droplet transportation with a tablet computer as the optical source, taking us closer to the goal of a portable optoelectrowetting lab-on-a-chip system.

B. Future Work

The significant reduction in droplet actuation voltage along with the enhanced capability of low voltage multi-axis manipulation using this OEWOD device is a step towards achieving a portable light-actuated digital microfluidic device. The threshold voltage can be further reduced by increasing the dielectric properties of the hydrophobic layer. Miniaturization of the voltage source will be critical in achieving device portability. We additionally plan to develop motion planning algorithms for automatically coordinating the motions of the droplets on the devices to create specified droplet formations.

ACKNOWLEDGMENTS

We thank the Optics Center cleanroom at UNC Charlotte, National Nanofabrication Facility at Georgia Tech, and Shared Materials Instrumentation Facility at Duke University for fabrication assistance.

REFERENCES

[1] D. Figeys and D. Pinto, "Lab-on-a-chip: A revolution in biological and medical sciences.," *Analytical Chemistry*, vol. 72, no. 9, pp. 330 A–335 A, 2000.

[2] M. G. Pollack, A. D. Shenderov, and R. B. Fair, "Electrowetting-based actuation of droplets for integrated microfluidics," *Lab Chip*, vol. 2, pp. 96–101, 2002.

[3] C. J. Kim, H. Moon, S. K. Cho, and R. L. Garrell, "Low voltage electrowetting-on-dielectric," *Journal of Applied Physics*, vol. 92, pp. 4080–4087, oct 2002.

[4] S. Y. Park and P. Y. Chiou, "Light-driven droplet manipulation technologies for lab-on-a-chip applications," *Advances in OptoElectronics*, vol. 2011, p. 12, aug 2011.

[5] G. Beni and S. Hackwood, "Electro-wetting displays," *Applied Physics Letters*, vol. 38, pp. 207–209, Feb. 1981.

[6] P. Y. Chiou, H. Moon, H. Toshiyoshi, C. J. Kim, and M. C. Wu, "Light actuation of liquid by optoelectrowetting," *Sensors and Actuators A: Physical*, vol. 104, no. 3, pp. 222–228, 2003.

[7] S. Y. Park, M. A. Teitell, and E. P. Y. Chiou, "Single-sided continuous optoelectrowetting (SCOEW) for droplet manipulation with light patterns," *Lab Chip*, vol. 10, no. 13, pp. 1655–1661, 2010.

[8] S. Y. Park, S. Kalim, C. Callahan, M. A. Teitell, and E. P. Y. Chiou, "A light-induced dielectrophoretic droplet manipulation platform," *Lab Chip*, vol. 9, no. 22, pp. 3228–3235, 2009.

[9] F. Arai, K. Onda, R. Iitsuka, and H. Maruyama, "Multi-beam laser micromanipulation of microtool by integrated optical tweezers," in *IEEE International Conference on Robotics and Automation*, (Kobe, Japan), pp. 1832–1837, 2009.

[10] F. Arai, K. Yoshikawa, T. Sakami, and T. Fukuda, "Synchronized manipulation and force measurement by optical tweezers using high-speed laser scanning," in *IEEE International Conference on Robotics and Automation*, (New Orleans, LA), pp. 890–895, Apr. 2004.

[11] J. J. Abbott, Z. Nagy, F. Beyeler, and B. J. Nelson, "Robotics in the small, Part I: Microrobotics," *IEEE Robotics and Automation Magazine*, vol. 14, no. 2, pp. 92–103, 2007.

[12] S. Hu and D. Sun, "Automatic transportation of biological cells with a robot-tweezer manipulation system," *International Journal of Robotics Research*, vol. 30, pp. 1681–1694, Dec. 2011.

[13] A. G. Banerjee, A. Pomerance, W. Losert, and S. K. Gupta, "Developing a stochastic dynamic programming framework for optical tweezer-based automated particle transport operations," *IEEE Transactions on Automation Science and Engineering*, vol. 7, no. 2, pp. 218–227, 2010.

[14] A. Ashkin and J. M. Dziedzic, "Optical levitation of liquid drops by radiation pressure," *Science*, vol. 187, no. 4181, pp. 1073–1075, 1975.

[15] N. Magome, M. I. Kohira, E. Hayata, S. Mukai, and K. Yoshikawa, "Optical trapping of a growing water droplet in air," *The Journal of Physical Chemistry B*, vol. 107, no. 16, pp. 3988–3990, 2003.

[16] A. A. Darhuber, J. P. Valentino, J. M. Davis, S. M. Troian, and S. Wagner, "Microfluidic actuation by modulation of surface stresses," *Applied Physics Letters*, vol. 82, no. 4, pp. 657–659, 2003.

[17] B. Selva, V. Miralles, I. Cantat, and M. C. Jullien, "Thermocapillary actuation by optimized resistor pattern: bubbles and droplets displacing, switching and trapping," *Lab Chip*, vol. 10, pp. 1835–1840, 2010.

[18] S. N. Pei, J. Valley, S. Neale, A. Jamshidi, H. Y. Hsu, and M. Wu, "Light-actuated digital microfluidics for large-scale, parallel manipulation of arbitrarily sized droplets," in *IEEE 23rd International Conference on Micro Electro Mechanical Systems (MEMS)*, pp. 252–255, Jan. 2010.

[19] E. J. Griffith and S. Akella, "Coordinating multiple droplets in planar array digital microfluidic systems," *International Journal of Robotics Research*, vol. 24, pp. 933–949, Nov. 2005.

[20] J. Ding, K. Chakrabarty, and R. Fair, "Scheduling of microfluidic operations for reconfigurable two-dimensional electrowetting arrays," *IEEE Transactions on Computer-Aided Design of Integrated Circuits and Systems,*, vol. 20, pp. 1463–1468, Dec. 2001.

[21] K. Bohringer, "Modeling and controlling parallel tasks in droplet-based microfluidic systems," *IEEE Transactions on Computer-Aided Design of Integrated Circuits and Systems,*, vol. 25, pp. 334–344, Feb. 2006.

[22] Z. Ma and S. Akella, "Coordination of droplets on light-actuated digital microfluidic systems," in *IEEE International Conference on Robotics and Automation*, (St. Paul, MN), pp. 2510–2516, May 2012.

[23] V. Shekar, M. Campbell, and S. Akella, "Towards automated optoelectrowetting on dielectric devices for multi-axis droplet manipulation." Video supplement, *IEEE International Conference on Robotics and Automation*, May 2013.

[24] T. B. Jones, "On the relationship of dielectrophoresis and electrowetting," *Langmuir*, vol. 18, no. 11, pp. 4437–4443, 2002.

[25] S. Park, C. Pan, T. H. Wu, C. Kloss, S. Kalim, C. E. Callahan, M. Teitell, and E. P. Y. Chiou, "Floating electrode optoelectronic tweezers: Light-driven dielectrophoretic droplet manipulation in electrically insulating oil medium," *Journal of Applied Physics*, vol. 92, no. 15, pp. 151101(1)–151101(3), 2008.